Five-Lipoxygenase-Activating Protein Mediated CYLD Attenuation is a Candidate Driver in Hepatic Malignant Lesion

Kun-kai Su
State Key Laboratory for Diagnosis and Treatment of Infectious Diseases, The First Affiliated Hospital, Zhejiang Unversity School of Medicine

Xue-hua Zheng
Institue of Pharmacology and Toxicology, College of Pharmaceutical Sciences, Zhejiang University

Christian Bréchot
Pasteur Institute: Institut Pasteur

Xiao-ping Zheng
Department of Pathology, Shulan (Hangzhou) Hospital

Dan-hua Zhu
State key Laboratory for Diagnosis and Treatment of Infectious Diseases, The First Affiliated Hospital, Zhejiang University School of Medcine

Rong Huang
Departmant of Pathology, Shulan (Hangzhou) Hospital

Yan-hong Zhang
State Key Laboratory for Diagnosis and Treatment of Infectious Diseases, The First Affiliated Hospital, Zhejiang Unversity School of Medcine

Jing-jing Tao
State Key Laboratory for Diagnosis and Treatment of Infectious Diseases, The First Affiliated Hospital, Zhejiang University School of Medcine

Yi-jia Lou
Institute of Pharmacology and Toxicology, College of Pharmaceutical Sciences, Zhejiang University

Lan-juan Li (ljli@zju.edu.cn)
State Key Laboratory of Diagnosis and Treatment of Infectious Diseases, The First Afflliated Hospital, Zhejiang University School of Medcine

Research Article

Keywords: Hepatocellular carcinoma, Lipid pro-inflammatory mediators, 5-lipoxygenase pathway, median survival time, candidate biomarker

Posted Date: November 30th, 2021

DOI: https://doi.org/10.21203/rs.3.rs-1103655/v1

Abstract

Background: Hepatocellular carcinoma (HCC) is an inflammation-associated cancer. However, the lipid pro-inflammatory mediators have only been seldom investigated in HCC pathogenesis. Activation of NF-κB and expression of c-Myc are negatively regulated by cylindromatosis (CYLD) in hepatocarcinogenesis. But it remains largely unknown whether lipid pro-inflammatory mediators are involved in CYLD suppression. Here, we aimed to evaluate the significance of hepatic lipid pro-inflammatory metabolites of arachidonate affected CYLD expression via 5-lipoxygenase (5-LO)-pathway.

Methods: Resection liver tissues from HCC patients or donors were evaluated for the correlation of 5-LO/cysteinyl leukotrienes (CysLTs)-signaling to expression of CYLD. The impact of functional components in 5-LO/CysLTs cascade on survival of HCC patients was subsequently assessed. Both livers from canines, a routine animal for drug safety evaluation, and genetic-modified human HCC cells treated with hepatocarcinogen aristolochic acid I (AAI) were further used to reveal the possible relevance between 5-LO pathway activation and CYLD depression.

Results: 5-LO-activating protein (FLAP), an essential partner of 5-LO, significantly overexpressed and was parallel to CYLD depression, CD34 neovascular localization, and high Ki-67 expression in the resection tissues from HCC patients. Importantly, high hepatic *FLAP* transcription markedly shortened the median survival time of HCC patients after surgical resection. In the livers of AAI-treated canines, FLAP overexpression was parallel to enhanced CysLTs contents, simultaneous attenuated CYLD expression. Moreover, knock-in *FLAP* significantly diminished the expression of CYLD in AAI-treated human HCC cells.

Conclusions: Hepatic FLAP/CysLTs axis is a crucial suppressor of CYLD in HCC pathogenesis, which highlights a novel mechanism in hepatocarcinogenesis and development. FLAP therefore can be explored for the early HCC detection and a target of anti-HCC therapy.

Background

Hepatocellular carcinoma (HCC) is one of the most lethal malignancies and the second cause of cancer death worldwide [1–3]. HCC surveillance is associated with early tumor detection and improved survival in patients with liver diseases [4]. To date, it is not full elucidated how initial molecular events and signaling involve the onset and progression of HCC. HCC is defined as an inflammation-associated cancer [5]. Hepatocarcinogenesis and progression may evolve from the inflammation. However, the lipid pro-inflammatory mediators have only been seldom investigated in HCC pathogenesis. Cysteinyl leukotrienes (CysLTs), that is LTC_4, LTD_4 and LTE_4, are lipid-signaling molecules that mediate both acute and chronic inflammation [6]. CysLTs constitute the major products of arachidonic acid (AA) metabolism via 5-lipoxygenase (5-LO) pathway [7, 8], that forming 5-LO/CysLTs cascade. The integral membrane protein 5-LO-activating protein (FLAP) is an essential partner of 5-LO for the first step in LTs synthesis [9, 10], it selectively transfers AA to 5-LO and enables the sequential oxygenation of AA [11]. Any factor inducing FLAP expression can lead to the enhancement of CysLTs synthesis. The primary metabolite

LTA_4 is further converted to LTC_4 via LTC_4 synthase (LTC_4S) or its isoenzyme, membrane-embedded microsomal glutathione-*S*-transferase 2 (mGST2) [12–14]. CysLTs bind at different affinities to two classical G-protein coupled receptors: CysLTR1 and CysLTR2 [8, 15] (Fig. 1). Activation of CysLTRs exerts downstream effects, including chemokine production, immune cell activation and tissue inflammation [16]. Cancer cells may utilize the 5-LO pathway to interact with tumor microenvironment during the development and progression of a tumor [8, 17]. Chemicals-induced liver damage in animal models displays the 5-LO-pathway activation and CysLTs content elevation [7, 18, 19]. And hepatitis B virus X protein enhances proliferation of hepatoma cells via AA metabolism associated pathways *in vitro* [20]. However, the underlying mechanism by which CysLTs contributes to HCC pathogenesis is so far not well documented. Whether 5-LO/CysLTs cascade also take a critical role in promoting hepatocarcinogenesis and development is still elusive.

Cylindromatosis (CYLD), a deubiquitination enzyme, negatively regulates cancer development and progression [21]. Livers in CYLD-deficient mice display spontaneous Kupffer cell activation, inflammatory cell infiltration, and nuclear factor (NF)-κB activation, or oncoprotein c-Myc expression and potentiated tumor development induced by diethylnitrosamine [22, 23]. CysLTs can initiate NF-κB constitutively active in up to 80% of colorectal tumors [24, 25]. However, it is still unclear whether 5-LO/CysLTs cascade is required for CYLD suppression. Understanding the relevance of 5-LO pathway to the CYLD expression, and the signal cooperativity might provide a deeper look into the initiation mechanism in hepatocarcinogenesis and HCC development.

Short-term aristolochic acid I (AAI) exposure leads to AAI-DNA adducts formation, NF-κB signaling activation and c-Myc expression in kidneys and livers of human *TP53* knock-in mice [26]. Owing to their biological nature, canines have become a routine animal in evaluating drug safety to predicate underlying toxicity profile in humans [27]. Our previous study confirms that hepatic premalignant lesion appears in canines after a 10-days AAI oral administration. It is featured by the overexpression of c-Myc and oncofetal RNA-binding protein Lin28B [28]. The premalignant node involves microRNAs dysregulation, as well as interleukin (IL)-6 receptor, p-STAT3, and NF-kB activation [28]. Therefore, it is extremely valuable to further explore whether 5-LO/CysLTs cascade is associated with AAI-induced hepatocarcinogenesis and involved in CYLD suppression.

In the present study, we report that FLAP highly expresses in the resection tissues from HCC patients. Furthermore, high transcription of *FLAP* in resection tissue significantly shortens the median survival time (MST) of HCC patients after surgical resection. Using an AAI-treated canine model and human HCC cell lines, we further highlight the potential role of hepatic FLAP/CysLTs cascade contributes to CYLD attenuation. This finding provides the hopeful target for early HCC detection and anti-HCC drug development.

Materials And Methods

Human Subjects

Human liver samples were collected from HCC patients undergoing surgical resection or liver transplantation, and healthy donors for liver transplantation in the form of histologic section at Shulan (Hangzhou) Hospital, China. Protocols for patient tissue collection were reviewed and approved by the ethics committees of Shulan (Hangzhou) Hospital, China (№ 20170207). Written informed consent was obtained. All experiments were done in accordance with the governmental and institutional guidelines of the ICH-GCP (according to the principles of the Declaration of Helsinki) and were performed under the written approval by the First Affiliated Hospital of Zhejiang University, China (№ 2018-327) and the Human Ethics Committee of Shulan (Hangzhou) Hospital. Histopathological grading was performed at the department of pathology in Shulan (Hangzhou) hospitals. All the participants that donated liver tissues are anonymized and summarized in **Suppl. Table S1.**

Animal Experimentation

Canine protocols were approved by the First Affiliated Hospital of Zhejiang University, College of Medicine, Zhejiang University, China (№ 2018-396) and all procedures were performed in accordance with the institutional guidelines. Ten-months-old male beagle canines were purchased from the ANNIMO Science and Technology and maintained in a specific pathogen-free environment.

AAI (purity > 98%, HPLC, Delta) was mixed with filler and filled into capsules. Canines were randomly assigned into two groups and given capsules with filler AAI filler (3 mg/kg/day [28]) or control for 10 days. Canines were sacrificed 11 days after initiation of the treatment. Livers were excised immediately after sacrifice. Part of the liver was fixed in 4% (wt/vol) neutral buffered formalin (pH 7.4) and embedded in paraffin for histologic analyses; the remaining liver was immediately snap-frozen in liquid nitrogen and kept at -80℃ until use.

Antibodies

Immunohistochemistry: Anti-FLAP (sc-28815), mGST2 (sc-65130), LTC_4S (sc-22564) were purchased from Santa Cruz Biotechnology (California, USA). CysLTR2 (ab32536) was purchased from Multisciences Biotech (Hangzhou, China). CYLD (#8462) was purchased from Cell Signaling Technology (Danvers, USA). 4',6'-diamidino-2-phenylindole (DAPI) (ZLI-9557) was purchased from Zhongshan Jinqiao Biotechnology (Beijing, China).

Western blot: Anti-FLAP, mGST2, LTC_4S, CysLTR2 and CYLD were the same as mentioned above. 5-LO (sc-8885) was purchased from Santa Cruz Biotechnology. LTB_4 receptor 1 (BLT1) (ab131041) and BLT2 (ab84600), were purchased from Abcam (Cambridge, England). CysLTR1 (ab32534) was purchased from Multisciences Biotech (Shanghai, China). Antibodies of c-Jun N-terminal kinase (JNK) (#9252), phospho-JNK (p-JNK) (#9251), eukaryotic translation initiation factor 2 alpha (eIF2a) (#2103), p-eIF2a (#3398), 78-kDa glucose-regulated protein (GRP78) (#3177), and 94 kDa Glucose-Regulated Protein (GRP94) (#2104) were purchased from Cell Signaling Technology. Microsomal prostaglandin E synthase-1 (mPGES-1) (#160140) was purchased from Cayman Chemical (Ann Arbor, USA). β-Actin (Mab1445), GAPDH (Mab5465-040), α-Tubulin (ab36864), β-Tubulin (ab012) and the HRP-conjugated secondary antibodies

(goat anti-mouse, LK-GAM007; goat anti-rabbit, LK-GAR007; and rabbit anti-goat, LK-RAG007) were purchased from Multisciences Biotech.

Histological assessments of liver tissues

Human liver paraffin-embedded consecutive 4 μm-thick sections were performed for immunohistochemical analysis. Anti-Ki-67 (IR098) and CD34 (IM034) were purchased from LBP (Guangzhou, China). Canine liver sections were prepared as described previously [28] for hematoxylin and eosin (H&E) or immunohistochemical stains, and consecutive 8 μm-thick frozen sections (cut by a freezing microtome, CM1950, Leica, Wetzlar, Germany) for immunofluorescent staining. Immunofluorescence analysis was performed using confocal microscopy (TCS SP8 MP, Leica). Both human and canine liver sections were stained with indicating antibodies to distinguish the immunohistochemical or immunofluorescence changes in expression and distribution *in situ*. For Ki-67 tissue evaluation, section was graded based on the percentage of Ki-67 positively stained nuclei, using the range 0~100 %.

Western blot analysis and ELISA

Western blot assay was performed as described previously [28]. Briefly, samples were homogenized with RIPA buffer (P0013K, Beyotime, Shanghai, China) for protein extraction. Whole blotting gel quantified with a fluorescence scanner imaging system (Bio-Rad, Hercules, California, USA) and densitometry was performed using Image J software (https://imagej.nih.gov/ij, NIH, Bethesda, MD, USA).

Supernatant containing CysLTs was extracted from liver tissue homogenate of canines (1:10 W:V, 50 mmol/L Tris-HCl, pH=7.5). CysLTs level was measured by ELISA Kit (Cayman, USA) on a DTX 880 Multimode Detector (Beckman Coulter, USA).

Bioinformatics analysis of gene transcriptions

MRNA sequencing data of HCC tissues and clinical follow-up record of HCC cohort were downloaded from The Cancer Genome Atlas (TCGA) in accordance with the data usage policy. MRNA expression of indicating genes was retrieved [29]. Patients were allocated into dichotomized subgroups based on processed expression for the survival analysis. Kaplan-Meier plots were used for comparison of survival curves, and log-rank tests were applied for *P*-values calculation.

Real-time qRT-PCR analysis

Real-time qRT-PCR analysis was conducted according to the protocol [30]. Briefly, total RNAs from human HCC cell lines were isolated with TRIzol reagent (Gibco BRL, USA). After 2 min of initial denaturation at 95°C, amplification used 40 cycles following 15 s at 95°C and 1 min at 60°C. The primer sequences (5’-3’) for *FLAP*, *Lta4h* (LTA_4 hydrolase) and *GAPDH* (in human HCC cells) were documented in Supplementary Table S2.

Cell culture, genetic-handling of *FLAP* in human HCC cells

The human HCC cell line HepG2, Hep3B2.1-7 and PLC/PRF/5 were purchased from Shanghai Institute of Cell Bank, Chinese Academy of Sciences (№ 22008). Cells were maintained in DMEM (12800-017, Life Technologies, USA) supplemented with 10% fetal bovine serum (FBS; 10099-141, Gibco, Germany).

Overexpression of *FLAP* in HepG2 cells was achieved by lentiviral infection. Lentivirus (lv) were constructed, concentrated and purified by Genechem (Shanghai, China). HepG2 cells were infected with lv-*Control* (lv-*Con*) or lv-*FLAP* (HepG2$^{lv\text{-}Con}$, HepG2$^{lv\text{-}FLAP}$) (MOI=10), and then selected for 3 days in the presence of 2.5 μg/ml puromycin (Gibco, Germany). Knockdown of *FLAP* in HepG2 cells was conducted by short hairpin RNA (shRNA). Sh-*FLAP* varietas and sh-*Con* plasmids (Sangon Biotech, Shanghai, China) were transfected with Lipofectamine 2000 transfection agent (HepG2$^{sh\text{-}FLAP}$, HepG2$^{sh\text{-}Con}$) (Invitrogen, Life Technologies) according to the manufacturer's instructions. Sequences for shRNA were shown in Supplementary Table S3. Lv-RNA or shRNA interfering efficiency was validated by qRT-PCR.

HepG2$^{lv\text{-}FLAP}$ and HepG2$^{sh\text{-}FLAP}$, and wild type (WT), HepG2$^{lv\text{-}Con}$ or HepG2$^{sh\text{-}Con}$ cells were further incubated with AAI (final concentration 1.25 μM) for another 7 days. Cells were harvested on day 10 after initiation of infection or transfection. The expression of FLAP in cells was examined by Flow cytometry according to commercial instruction. Finally, cells were analyzed by a BD FACSCount II Flow Cytometer (BD Biosciences, San Jose, USA).

Statistical analysis

Pairwise comparisons between continuous data were analyzed using an unpaired two-tailed Student *t* test, and multiple comparisons were analyzed by one-way ANOVA. All data were expressed as mean ± SD, and $P < 0.05$ were considered statistically significant. Significant *P* values are indicated by asterisks in the individual figures.

Results

FLAP overexpression is paralleled to CYLD suppression inresectiontissues fromHCC patients

We explored the impact of functional components in CysLTs biosynthesis on CYLD expression in the resection tissues from ten HCC patients. The overview diagram of CysLTs biosynthesis exhibits AA metabolism through 5-LO pathway (**Fig 1**). To investigate the involvement of FLAP in the progression of HCC, we examined its expression and localization in the resection tissues. Patients' characteristics were summarized, concerning etiology, gender, age, and tumor stage (**Suppl. Table S1**). Immunohistochemical staining revealed that FLAP level was considerable higher in the resection tissues from HCC patients as compared to the samples from donor controls (**Fig. 2a, upper left panel**). All the HCC resection tissues displayed the higher FLAP expression, but only one in ten liver tissues from donors expressed marginal FLAP (**Fig. 2b**). In contrast, the resection tissues from HCC patients had markedly lower CYLD expression than the samples from donor controls (**Fig. 2a, bottom right panel**). Considering that both mGST2 and

CysLTR2 in 5-LO pathway were basically required in the lipid pro-inflammatory mediators signaling transduction, we subsequently observed their abundance, and further clustered all the four molecular events according to their expression grades in resection tissues from HCC patients or donors (**Fig. 2a, Fig 2b**). In parallel to high FLAP expression, eight in ten resection HCC tissues showed absence of CYLD expression (**Fig. 2b**). As to the two cases with CYLD expression, one showed CYLD nuclear translocation together with a much higher cytosolic CysLTR2 expression within poorly differentiated HCC lesions (**Suppl. Fig. 1, left panel**), and the other one displayed slight cytosolic CYLD expression together with a much higher nuclear CysLTR2 expression in paracancerous tissue (**Suppl. Fig. 1, right panel**). Furthermore, compared to the ratio of overexpression of mGST2 (3/10) and CysLTR2 (2/10) in donor livers, there are much more overexpression of mGST2 (8/10) and CysLTR2 (10/10) in HCC tissues (**Fig. 2b**). According to the clustered results, the hepatic mGST2 and CysLTR2 have a basal expression level under the physiological condition, but their expressions robustly enhanced in malignant lesion, depending on the upstream element FLAP level. Strikingly, there was less significance of high expressions of mGST2 and CysLTR2 to CYLD suppression in the livers of donors, implying that mGST2 and CysLTR2 was not prerequisite for inhibiting CYLD expression. Our data strongly suggested a negative correspondence between FLAP overexpression and CYLD attenuation in HCC tissues (**Fig 2b**), suggesting that overexpressed FLAP was a potential hallmark of HCC. We further identified the effects of overexpressed FLAP on HCC invasiveness and development, as evidenced by evaluating the downstream effectors. We found that CD34, the marker of hematopoietic stem cells, as well as Ki-67, the marker of cell proliferation, highly expressed in resection tissues of HCC contrast to donors (**Fig 2c**). In 6 in10 resection tissues of HCC showed CD34 neovascular localization (including tumor angiogenesis), and in 9 in10 resection tissues of HCC showed Ki-67 overexpression (**Fig 1d and Suppl. Table S1**). Importantly, the HCC tissues exhibited FLAP overexpression with ++ grades (≥50% positive rate) also showed Ki-67 expression with ++ grades. In contrast, the donor livers without FLAP expression showed neither CD34 nor Ki-67 expression (**Fig 1d**). These data implied that overexpressed FLAP was correlated with CYLD suppression, and involved in neovascularization and tumor cell proliferation in HCC tissues. Therefore, our findings that hepatic FLAP increased in expression could be a valuable target for both therapeutics and predicting survival of HCC patients after surgical resection.

Enhanced *FLAP* transcription shortens the median survival time of HCC patients after surgical resection

To support the evidences for the role of FLAP on the clinical findings described above, we took advantage of the long-term clinical follow-up information provided by The Cancer Genome Atlas (TCGA) for bioinformatics analysis. We obtained a 417 HCC cohort, which was well documented with survival information. We subsequently analyzed the relationships between the transcription levels of hepatic *FLAP*, *mGST2*, *CysLTR1, CysLTR2, CYLD* and the MST in HCC patients after surgical resection, respectively. Notably, MST was only 47 months for high *FLAP* mRNA in HCC patients (P=0.04) contrasted to 104 months for low *FLAP* mRNA (**Fig 3a**). Conversely, there was only slighter effect between high and low *mGST2* mRNA on MST in HCC patients (P=0.27) after surgical resection (**Fig 3b**). On the other hand, higher *CysLTR2* mRNA significantly shortened MST in HCC patients (P=0.04) after surgical resection (**Fig 3c**). Further, MST was as low as 34 months for low *CYLD* mRNA and 56 months for high *CYLD* mRNA in

HCC patients after surgical resection (P=0.04) (**Fig 3d**). Remarkably, the effects of hepatic *FLAP* or *CysLTR2* and *CYLD* transcription on MST also displayed a negative correlation in HCC patients after surgical resection. Obviously, the patients with low *FLAP* mRNA had a much longer survival period (MST 104 month) than those with low *CysLTR2* mRNA (MST 84 month), indicating that the transcription level of *FLAP* is one of the most crucial impacts on survival of HCC patients after surgical resection. From the MST point of view, enhanced *FLAP* appeared much earlier than attenuated *CYLD* in HCC patients (**Fig 3a, 3d**), therefore, FLAP possessed the crucial value to evaluate the progress and recrudesce of HCC patients after surgical resection.

Hepatic CYLD attenuation and CysLTs increasement after AAI treatment

To determine whether 5-LO/CysLTs cascade influence CYLD depression, we first assessed the effect of AAI on CYLD expression in livers of canines. Compared to control, both the abundance of CYLD in hepatocytes and the numbers of CYLD-positive hepatocytes by AAI treatment extremely decreased using immunofluorescence staining (**Fig 4a**). Western blot analysis further confirmed that AAI treatment significantly attenuated the expression of CYLD in liver tissues (**Fig 4b**). Next, H&E stained liver sections displayed inflammatory cell infiltration round central veins after AAI treatment (**Fig 4c**), which was similar to the feature spontaneously appeared in the livers of CYLD-deficient mice [31]. We then further examined the effect of AAI on CysLTs biosynthesis in canine livers. As determined by ELISA, AAI treatment significantly raises the content of CysLTs in liver homogenate supernatant compared to control (**Fig 4d**). These data suggested that CysLTs generation was paralleled to CYLD attenuation accompanied by the CYLD-deficient feature of inflammatory cell infiltration round central veins in AAI-treated canine livers.

Hepatic FLAP overexpression contributes to CysLTs increase

To obtain functional insights on hepatic 5-LO/CysLTs cascade in AAI-induced CYLD suppression, we observed the expression of each component in 5-LO pathway. Using Western blotting, we evaluated the expressions of 4 catalytic proteins involved in LTC_4 biosynthetic process, and found that FLAP and mGST2 were significantly higher in expression compared to control (P<0.01, P<0.05, respectively) in AAI-treated liver (**Fig 5a**). Particularly, we individually identified the abundance and distribution of each protein involved in LTC_4 biosynthesis in the liver tissues with immunohistochemical staining. We observed that, compared to control, AAI induced considerable overexpression of FLAP in both hepatocytes and Kupffer cells. MGST2 highly expressed in hepatocytes, but LTC_4S did not change in expression by AAI treatment (**Fig 5b**, the positive or negative control for immunohistochemical analysis seen **Suppl Fig. 2**). In contrast, AAI failed to increase the transcription of hepatic *Lta4h* at LTA_4–derived LTB_4 step in the 5-LO bypass (**Fig 5c**) [32]. Conversely, AAI significantly inhibited the expression of hepatic mPGES-1 (P<0.05) (**Fig 5a, b**), which catalyzes prostaglandin (PG) E_2 generation at the terminal steps of cyclooxygenase (COX)-pathway. These data indicated that neither 5-LO/LTB_4 bypass nor COX/PGE_2 pathway contributed to AAI-induced hepatic CYLD suppression. Therefore, AAI treated-livers underwent FLAP/CysLTs cascade associated pathogenesis.

Endoplasmic reticulum stress contributes to CysLTs/CysLTR2 signaling transduction

To understand the underlying molecular mechanism of CysLTs-associated with CYLD attenuation after AAI treatment, we subsequently focused on the connection of CysLTs/CysLTRs signaling in canine livers. Meanwhile, we also checked endoplasmic reticulum (ER) stress, since ER stress inducers showed the ability to reduce CYLD expression [33]. We detected the expressions of CysLTR1, CysLTR2, BLT1 (the high-affinity receptor of LTB_4), BLT2, Grp78, Grp 94 (the early events of ER stress), as well as phosphorylation of eIF2α (the late event of ER stress) once stimulated with AAI. We observed that, compared to control, AAI significantly upregulated CysLTR2 expression (P<0.05), but did not influence on the expressions of CysLTR1 (**Fig. 6a**), BLT1 and BLT2 (**Suppl. Fig. 3**). These data indicated that, among the hepatic receptors associated with LTs, only CysLTR2 displayed overexpression in response to AAI treatment. Furthermore, AAI increased both high expression of Grp78 (P<0.05) and phosphorylation of eIF2α (P<0.01) (**Fig. 6b**), suggesting that a possible relevance existed in ER stress and CysLTR2 activation. We next measured the phosphorylation of JNK, one of the downstream effectors of the CYLD attenuation, and found that JNK was significantly phosphorylated (P<0.01) (**Fig. 6c**). Taken together, AAI induced high expression of CysLTR2 was accompanied by ER stress and phosphorylation of JNK, implying that ER stress/CysLTR2 axis probably promoted the FLAP/CysLTs/CYLD/p-JNK signaling transduction in AAI-treated livers.

Knock-in *FLAP* diminishes CYLD expression inHepG2 cells

To further confirm the impact of FLAP on CYLD expression, we explored the abundance of CYLD in WT, lv-*FLAP*, and sh-*FLAP* human HCC cell lines according to the scheme of the experimental procedure (**Fig 7a**). Among human HCC cell line HepG2, Hep3B and PLC/PRF/5, we validated the favorable nature of FLAP expression in HepG2 cells in response to AAI exposure (**Fig 7b**). We therefore modulated the abundance of FLAP in HepG2 cells to generate $HepG2^{lv\text{-}FLAP}$ or $HepG2^{sh\text{-}FLAP1}$, $HepG2^{sh\text{-}FLAP2}$ cells. Compared to WT, $HepG2^{lv\text{-}Con}$ or $HepG2^{sh\text{-}Con}$ cells, we observed that either *FLAP* mRNA or FLAP-positive ($FLAP^+$) cell ratio were remarkable high in $HepG2^{lv\text{-}FLAP}$ cells (P<0.01), and decreased in $HepG2^{sh\text{-}FLAP}$ cells (P<0.01) using qRT-PCR (**Suppl. Fig. 4**) or flow cytometry assays (**Fig 7c**), indicating that infection or transfection efficiency was significant. Notably, there was an associated reduction of CYLD in $HepG2^{lv\text{-}FLAP}$ cells in compared to WT and $HepG2^{lv\text{-}Con}$ cells (P<0.05), while the expression of CYLD in $HepG2^{sh\text{-}FLAP2}$ cells was significantly higher than WT and $HepG2^{sh\text{-}Con}$ cells (P<0.05), as evidenced by Western blot assay (**Fig 7d, e**). These results intensively revealed that FLAP was required for negatively regulating CYLD expression in AAI-treated human HCC cells. Given that CysLTR2 more expressed in the tumor vasculature compared to CysLTR1 [34], we further evaluated CysLTR2 expression in WT, $HepG2^{lv\text{-}FLAP}$ or $HepG2^{sh\text{-}FLAP}$ cells. Unlike AAI-treated livers of canines, CysLTR2 did not change in expression in $HepG2^{lv\text{-}FLAP}$ or $HepG2^{sh\text{-}FLAP}$ cells in contrast to WT, $HepG2^{lv\text{-}Con}$ and $HepG2^{sh\text{-}Con}$ cells (**Fig 7d, e**). These data implied that HepG2 cells probably only kept limited expression of CysLTR2, and that its abundance was not significantly affected by FLAP. We suggested that the inherent CysLTR2 was enough to make CysLTs signal transduction, thereby negatively modulating CYLD expression. Schematic representation of

hepatic FLAP/CysLTs cascade contributing to the attenuation of CYLD in AAI-induced hepatic malignant alterations was illustrated in **Figure 7f**.

Discussion

The prognosis of HCC patients is poor, with only limited treatment options [35]. There is an urgent need to seek novel targets for the early diagnostic and preventive strategies of HCC patients. Hepatocarcinogenesis and development are a multistep process, and probably evolves from the inflammation. In the current study, we reveals that all the resection tissues from HCC patients show significant overexpression of FLAP in both malignant lesion and paracarcinoma tissues in contrast to those from donors. Further, FLAP is closely associated with neovascularization (including tumor angiogenesis) and cell proliferation in resection tissues of HCC patients, evidenced by high expression of FLAP or Ki-67, and neovascular localization of CD34 in parallel. Remarkably, the effect of mRNA level of hepatic *FLAP* on MST also displayed a close correlation in HCC patients after surgical resection. Of additional interest is that high transcription of *FLAP* leads to significantly shortening the MST of HCC patients after surgical resection, indicating that FLAP high expression does take a crucial role in HCC development or recrudesce.

By studying the impact of AAI treatment on 5-LO/CysLTs cascade, and further insights into the mechanism that links FLAP to CYLD in canine liver, we identify a novel candidate driver for hepatic malignant lesion. Following AAI administration of canines, the livers show a significant overexpression of FLAP accompanied by markedly higher CysLTs content. The enhanced hepatic FLAP/CysLTs cascade displays a negative correspondence to CYLD expression, and positive correspondence to its downstream effecter JNK phosphorylation. The present study reveals that both 5-LO/LTB_4 bypass and COX/PGE_2 pathway in AAI-treated livers of canines do not change in expression, indicating that both pathways less contributes to generation of the lipid pro-inflammatory mediators [32]. These data convincingly indicate that the more reduced CYLD is in association with increased CysLTs. Most importantly, the data from both $HepG2^{lv-FLAP}$ and $HepG2^{sh-FLAP}$ cells directly confirm the impact of FLAP abundance on CYLD expression after AAI treatment. The *in vitro* results intensively support that hepatic FLAP overexpression is required for suppressing CYLD. Strikingly, our study highlights the fact that enhanced hepatic FLAP/CysLTs cascade is involved in CYLD suppression. In the liver, CYLD acts as an important regulator of hepatocyte homeostasis [23]. In HCC pathogenesis, CYLD is involved in negatively regulating apoptosis, regeneration, NF-κB signaling, and inflammation. Consistent with our previous findings, such as apoptosis, regeneration, NF-κB signaling, and inflammation, in AAI-treated livers of canines [28], here, the further evidence that AAI-induced CYLD suppression accompanies the inflammatory cell infiltration round the central veins is quite similar to the features of spontaneously appeared in the livers of CYLD-deficient mice [31]. Owing to the FLAP overexpression-induced CYLD suppression, we consider that the hepatocyte homeostasis suffers from significant disorders, including all the features described above and the malignant progression in canine livers.

Conversely, the higher abundances of hepatic mGST2 and CysLTR2 do not cooperate with CYLD suppression in donors, although both highly express in the HCC tissues, similar to the livers in AAI-treated canines. Furthermore, the overexpression of mGST2 mRNAs does not influence the MST of HCC patients after surgical resection, suggesting that it is at least not involved in inhibiting expression of CYLD. These results intensively indicate that FLAP itself, rather than mGST2 and CysLTR2, is crucially important to HCC development and recrudesce in patients and AAI-induced hepatocarcinogenesis in canines. The compelling findings highlight the possible therapeutic implications of FLAP in human HCC development. Therefore, FLAP overexpression is a noteworthy index parameter running throughout the initiation and terminal in liver cancer pathology.

In rat liver, hepatocytes accounted for the highest ability to metabolize and produce CysLTs from the LTA_4 [36]. Using the FLAP as a marker, we confirm that FLAP overexpress in both hepatocytes and Kupffer cells in canine liver after AAI treatment. Since LTC_4S only expresses in cells of hematopoietic lineage, the present study does not show it highly expresses in canine livers, we believe that CysLTs in major come from hepatocytes. Given that FLAP aids to catalyze LTA4 production, our data reveal that AAI-induced overexpression of FLAP is the major element contributing to CysLTs generation in canine livers. Hepatocyte-derived CysLTs mediate hepatic vascular tone abnormalities in cirrhosis [37]. Five-LO pathway has been indicated to have a role in different cancers [38]. CysLTs involve the microenvironment, influencing local risk of malignant transformation [39]. To date, the signaling effects of CysLTs/CysLTR2 on oncogenesis and development are controversial. High CysLTR2 expression is correlated with a good prognosis in patients with colorectal cancer [40] and breast cancer [41]. But constitutive activation of CysLTR2 in uveal melanoma acts as an oncogene [42]. CysLTR2 expression in stromal cells, rather than tumor cells, is essential for enhanced invasiveness [34]. Although high expression of CysLTR2 appears in resection tissues of HCC patients and in AAI-induced premalignant livers of canines, the data from both $HepG2^{lv-FLAP}$ and $HepG2^{sh-FLAP}$ cells do not demonstrate the impact of FLAP abundance on CysLTR2 expression. We therefore focus on the hepatic ER stress/CysLTRs axis as ER stress triggers CysLTRs internalization [14] and ER stress inducers show the ability to reduce CYLD expression [33]. Our data demonstrate that AAI treatment triggers the early and late events of ER stress in canine livers, as evidenced by high Grp78 expression and of eIF2α phosphorylation, thereby promoting CysLTR2 internalization. Of CysLTs, LTC_4, LTD_4, and LTE_4 interacts their own specific receptors. LTC_4 possesses CysLTR2 specific affinity and potency [16]. LTC_4 is the only intracellular CysLT, it also outputs and exists in the extracellular space with very short lifetime. ER stress induces CysLTR2 internalization, making LTC_4 much easier to activate CysLTR2 intracellularly. Our results confirm a high FLAP expression involves in CysLTs generation *in vivo*. Once ER stress triggers CysLTR2 internalization, increased CysLTs have the strong tendency to let CysLTR2 activation. We consider that it is enough for CysLTs/CysLTR2 signaling transduction to take a local or transient effect on inhibiting CYLD expression in liver cancer pathology. Hepatic ER stress/CysLTR2 axis probably contributes to the FLAP/CysLTs/CYLD/p-JNK signaling transduction *in vivo*.

Nuclear expressions of CysLTRs are potential prognostic indicators of colorectal cancer. High CysLTR2 nuclear expression had the best survival expectancy [40]. Our data show that a high FLAP expression and high CysLTR2 nuclear expression results in CYLD expression in paracarcinoma tissues, while a high FLAP expression and high cytosolic CysLTR2 expression leads to CYLD nuclear translocation in malignant lesion. Although our data link CysLTR2 nuclear distribution to CYLD expression in HCC, we cannot confirm the contribution whether CysLTR2 distribution directly affects CYLD expression from the only two HCC patients.

Strikingly, we reveal that FLAP overexpression is correlated with CD34 neovascular localization and high Ki-67 expression in HCC tissues of HBV-infected patients. That means, once hepatic FLAP is detected and inhibited, neovascularization and tumor cell proliferation can probably be inhibited in HCC tissues. Recently, it has been highlighted to target 5-LO-pathway as a hopeful direction of therapy in different diseases [8, 9, 43]. Our data intensively suggest that no matter the resection tissues from HCC patients or AAI-induced premalignant lesion in canine livers share the same characteristics, that is, FLAP overexpression in parallel to CYLD attenuation. Based on our knowledge, we report here for the first time FLAP overexpression exists throughout the hepatic premalignant and the terminal HCC period. FLAP inhibition, therefore, may provide the foundation for new therapeutic strategies of HCC patients and possesses more meaningful for prolong life span of HCC patients after surgical resection.

Conclusions

In conclusion, as reported in Fig. 7f, we found that hepatic FLAP/CysLTs axis is a crucial suppressor of CYLD in HCC pathogenesis, which highlights a novel mechanism in hepatocarcinogenesis and development. FLAP therefore can be explored for the early HCC detection and a target of anti-HCC therapy.

Abbreviations

HCC, hepatocellular carcinoma; MST, median survival time; 5-LO, 5-lipoxygenase; FLAP, five-LO-activating protein; mGST2, microsomal glutathione-*S*-transferase 2; CysLTs, cysteinyl leukotrienes; CysLTRs, cysteinyl leukotrienes receptors; CYLD, cylindromatosis; AAI, aristolochic acid I.

Declarations

Ethics approval and consent to participate

Animal and/or human procedures were in compliance with the national and international directives and approved by The Human Ethics Committee of Shulan (Hangzhou) Hospital (№ 20170207), and The First Affiliated Hospital of Zhejiang University, College of Medicine, Zhejiang University, China (№ 2018-396 for animal and № 2018-327 for human).

Consent for publication

Not applicable.

Availability of data and materials

The datasets used and/or analysed during the current study are available from the corresponding author on reasonable request.

Competing interests

None declared.

Funding

This work is supported by the National Key Research and Development Program of China (2019YFC0840609 to Su. K), National Natural Science Foundation of China (№ 81401707 to Su K., № 81790630 to Li L., and № 91229124 to Lou Y.), and the Zhejiang Provincial Natural Science Foundation (№ LY20H030006 to Su K.).

Authors' Contributions

Su K. designed and conducted clinical data and *in vitro* experiments, bioinformatics analysis, statistical analysis, and drafted the manuscript. Zheng X. conducted most of the animal experiments and data analysis. Bréchot C. provided guidance on conception, reviewed and edited the manuscript. Zheng X. and Huang R. conducted the acquisition of clinical data of HCC patients and donors. Zhu D. and Tao J. aided to bioinformatics analysis. Lou Y. and Zhang Y. organized the animal study and acquisition of animal data. Li L provided guidance on conception, supervised the study for clinicopathological feature and pathological analysis of HCC patients, and final approval of the version to be published.

Acknowledgements

Bang-xin Chen aided Western blotting experiments. Data were eligible for HCC patient survival analysis in Figure 3 from the TCGA Research Network: http://cancergenome.nih.gov/.

References

1. Bertuccio P, Turati F, Carioli G, Rodriguez T, La Vecchia C, Malvezzi M, et al. Global trends and predictions in hepatocellular carcinoma mortality. J Hepatol 2017, 67:302-9.
2. Forner A, Reig M, Bruix J Hepatocellular carcinoma. Lancet 2018, 391:1301-14.
3. Wei Y, Chen X, Liang C, Ling Y, Yang X, Ye X, et al. A Noncoding Regulatory RNAs Network Driven by Circ-CDYL Acts Specifically in the Early Stages Hepatocellular Carcinoma. Hepatology 2020, 71:130-47.
4. Singal A G, Tiro J A, Murphy C C, Marrero J A, McCallister K, Fullington H, et al. Mailed outreach invitations significantly improve HCC surveillance rates in patients with cirrhosis: a randomized

clinical trial. Hepatology 2019, 69:121-30.

5. Gougelet A Epigenetic modulation of immunity: towards new therapeutic avenues in hepatocellular carcinoma? Gut 2019, 68:1727-8.
6. Di Gennaro A, Araujo A C, Busch A, Jin H, Wagsater D, Vorkapic E, et al. Cysteinyl leukotriene receptor 1 antagonism prevents experimental abdominal aortic aneurysm. Proc Natl Acad Sci U S A 2018, 115:1907-12.
7. Brenner C, Galluzzi L, Kepp O, Kroemer G Decoding cell death signals in liver inflammation. J Hepatol 2013, 59:583-94.
8. Wang D, Dubois R N Eicosanoids and cancer. Nat Rev Cancer 2010, 10:181-93.
9. Evans J F, Ferguson A D, Mosley R T, Hutchinson J H What's all the FLAP about?: 5-lipoxygenase-activating protein inhibitors for inflammatory diseases. Trends Pharmacol Sci 2008, 29:72-8.
10. Garscha U, Voelker S, Pace S, Gerstmeier J, Emini B, Liening S, et al. BRP-187: A potent inhibitor of leukotriene biosynthesis that acts through impeding the dynamic 5-lipoxygenase/5-lipoxygenase-activating protein (FLAP) complex assembly. Biochem Pharmacol 2016, 119:17-26.
11. Mandal A K, Skoch J, Bacskai B J, Hyman B T, Christmas P, Miller D, et al. The membrane organization of leukotriene synthesis. Proc Natl Acad Sci U S A 2004, 101:6587-92.
12. Ahmad S, Niegowski D, Wetterholm A, Haeggstrom J Z, Morgenstern R, Rinaldo-Matthis A Catalytic characterization of human microsomal glutathione S-transferase 2: identification of rate-limiting steps. Biochemistry 2013, 52:1755-64.
13. Burke L, Butler C T, Murphy A, Moran B, Gallagher W M, O'Sullivan J, et al. Evaluation of cysteinyl leukotriene signaling as a therapeutic target for colorectal cancer. Front Cell Dev Biol 2016, 4:103.
14. Dvash E, Har-Tal M, Barak S, Meir O, Rubinstein M Leukotriene C4 is the major trigger of stress-induced oxidative DNA damage. Nat Commun 2015, 6:10112.
15. Thompson C, Cloutier A, Bosse Y, Thivierge M, Gouill C L, Larivee P, et al. CysLT1 receptor engagement induces activator protein-1- and NF-kappaB-dependent IL-8 expression. Am J Respir Cell Mol Biol 2006, 35:697-704.
16. Austen K F, Maekawa A, Kanaoka Y, Boyce J A The leukotriene E4 puzzle: finding the missing pieces and revealing the pathobiologic implications. J Allergy Clin Immunol 2009, 124:406-14.
17. Roos J, Grosch S, Werz O, Schroder P, Ziegler S, Fulda S, et al. Regulation of tumorigenic Wnt signaling by cyclooxygenase-2, 5-lipoxygenase and their pharmacological inhibitors: A basis for novel drugs targeting cancer cells? Pharmacol Ther 2016, 157:43-64.
18. Su K, Wang Q, Qi L, Hua D, Tao J, Mangan C J, et al. Microrna-674-5p/5-lo axis involved in autoimmune reaction of concanavalin a-induced acute mouse liver injury. Toxicol Lett 2016, 258:101-7.
19. Titos E, Claria J, Planaguma A, Lopez-Parra M, Gonzalez-Periz A, Gaya J, et al. Inhibition of 5-lipoxygenase-activating protein abrogates experimental liver injury: role of Kupffer cells. J Leukoc Biol 2005, 78:871-8.

20. You X, Liu F, Zhang T, Li Y, Ye L, Zhang X Hepatitis B virus X protein upregulates oncogene Rab18 to result in the dysregulation of lipogenesis and proliferation of hepatoma cells. Carcinogenesis 2013, 34:1644-52.
21. Sun S C CYLD: a tumor suppressor deubiquitinase regulating NF-kappaB activation and diverse biological processes. Cell Death Differ 2010, 17:25-34.
22. Pannem R R, Dorn C, Ahlqvist K, Bosserhoff A K, Hellerbrand C, Massoumi R CYLD controls c-MYC expression through the JNK-dependent signaling pathway in hepatocellular carcinoma. Carcinogenesis 2014, 35:461-8.
23. Nikolaou K, Tsagaratou A, Eftychi C, Kollias G, Mosialos G, Talianidis I Inactivation of the deubiquitinase CYLD in hepatocytes causes apoptosis, inflammation, fibrosis, and cancer. Cancer Cell 2012, 21:738-50.
24. Hashimoto K, Ichiyama T, Hasegawa M, Hasegawa S, Matsubara T, Furukawa S Cysteinyl leukotrienes induce monocyte chemoattractant protein-1 in human monocyte/macrophages via mitogen-activated protein kinase and nuclear factor-kappaB pathways. Int Arch Allergy Immunol 2009, 149:275-82.
25. Kawano T, Matsuse H, Kondo Y, Machida I, Saeki S, Tomari S, et al. Cysteinyl leukotrienes induce nuclear factor kappa b activation and RANTES production in a murine model of asthma. J Allergy Clin Immunol 2003, 112:369-74.
26. Arlt V M, Zuo J, Trenz K, Roufosse C A, Lord G M, Nortier J L, et al. Gene expression changes induced by the human carcinogen aristolochic acid I in renal and hepatic tissue of mice. Int J Cancer 2011, 128:21-32.
27. Colagiovanni D B, Borkhataria D, Looker D, Schuler D, Bachmann C, Sagelsdorff P, et al. Preclinical 28-day inhalation toxicity assessment of s-nitrosoglutathione in beagle dogs and Wistar rats. Int J Toxicol 2011, 30:466-77.
28. Jin K, Su K K, Li T, Zhu X Q, Wang Q, Ge R S, et al. Hepatic premalignant alterations triggered by human nephrotoxin aristolochic acid I in canines. Cancer Prev Res (Phila) 2016, 9:324-34.
29. Cancer Genome Atlas Research Network. Electronic address w b e, Cancer Genome Atlas Research N Comprehensive and integrative genomic characterization of hepatocellular carcinoma. Cell 2017, 169:1327-41 e23.
30. Ogawa S, Tagawa Y, Kamiyoshi A, Suzuki A, Nakayama J, Hashikura Y, et al. Crucial roles of mesodermal cell lineages in a murine embryonic stem cell-derived in vitro liver organogenesis system. Stem Cells 2005, 23:903-13.
31. Martinez-Clemente M, Ferre N, Gonzalez-Periz A, Lopez-Parra M, Horrillo R, Titos E, et al. 5-lipoxygenase deficiency reduces hepatic inflammation and tumor necrosis factor alpha-induced hepatocyte damage in hyperlipidemia-prone ApoE-null mice. Hepatology 2010, 51:817-27.
32. Serezani C H, Lewis C, Jancar S, Peters-Golden M Leukotriene B4 amplifies NF-kappaB activation in mouse macrophages by reducing SOCS1 inhibition of MyD88 expression. J Clin Invest 2011, 121:671-82.

33. Yamashita S, Matsuo Y, Tawara N, Hara K, Yamamoto M, Nishikami T, et al. CYLD dysregulation in pathogenesis of sporadic inclusion body myositis. Sci Rep 2019, 9:11606.
34. Duah E, Teegala L R, Kondeti V, Adapala R K, Keshamouni V G, Kanaoka Y, et al. Cysteinyl leukotriene 2 receptor promotes endothelial permeability, tumor angiogenesis, and metastasis. Proc Natl Acad Sci U S A 2019, 116:199-204.
35. Cotton R T, Tran Cao H S, Rana A A, Sada Y H, Axelrod D A, Goss J A, et al. Impact of the Treating Hospital on Care Outcomes for Hepatocellular Carcinoma. Hepatology 2018, 68:1879-89.
36. Medina J F, Haeggstrom J, Kumlin M, Radmark O Leukotriene A4: metabolism in different rat tissues. Biochim Biophys Acta 1988, 961:203-12.
37. Titos E, Claria J, Bataller R, Bosch-Marce M, Gines P, Jimenez W, et al. Hepatocyte-derived cysteinyl leukotrienes modulate vascular tone in experimental cirrhosis. Gastroenterology 2000, 119:794-805.
38. Moore G Y, Pidgeon G P Cross-talk between cancer cells and the tumour microenvironment: the role of the 5-lipoxygenase pathway. Int J Mol Sci 2017, 18(2).
39. Wasilewicz M P, Kolodziej B, Bojulko T, Kaczmarczyk M, Sulzyc-Bielicka V, Bielicki D, et al. Overexpression of 5-lipoxygenase in sporadic colonic adenomas and a possible new aspect of colon carcinogenesis. Int J Colorectal Dis 2010, 25:1079-85.
40. Magnusson C, Mezhybovska M, Lorinc E, Fernebro E, Nilbert M, Sjolander A Low expression of CysLT1R and high expression of CysLT2R mediate good prognosis in colorectal cancer. Eur J Cancer 2010, 46:826-35.
41. Magnusson C, Liu J, Ehrnstrom R, Manjer J, Jirstrom K, Andersson T, et al. Cysteinyl leukotriene receptor expression pattern affects migration of breast cancer cells and survival of breast cancer patients. Int J Cancer 2011, 129:9-22.
42. Slater K, Hoo P S, Buckley A M, Piulats J M, Villanueva A, Portela A, et al. Evaluation of oncogenic cysteinyl leukotriene receptor 2 as a therapeutic target for uveal melanoma. Cancer Metastasis Rev 2018, 37:335-45.
43. Haeggstrom J Z Leukotriene biosynthetic enzymes as therapeutic targets. J Clin Invest 2018, 128:2680-90.

Figures

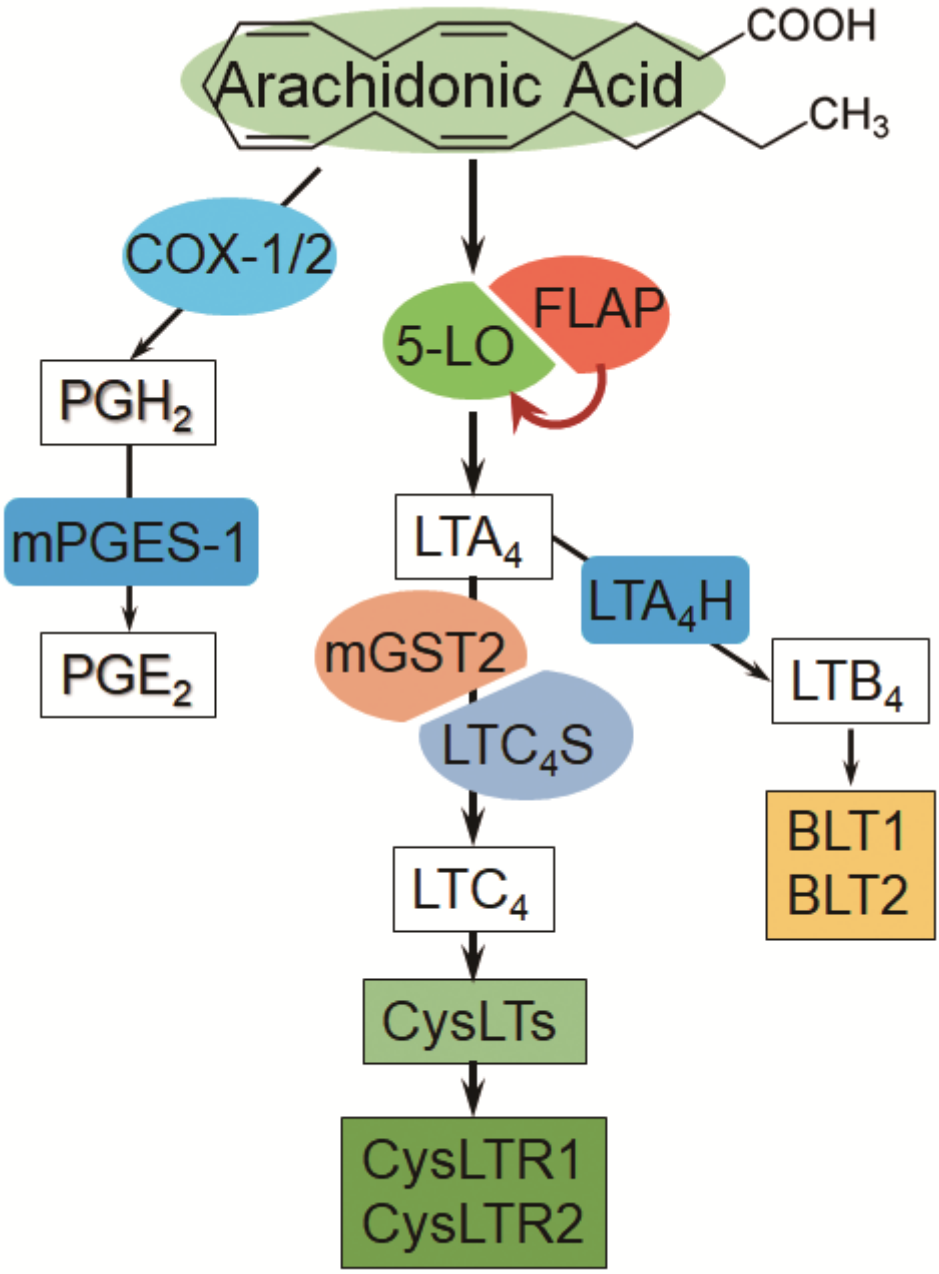

Figure 1

The overview diagram of arachidonic acid-derived metabolites pathways. In the left: COX/PGs pathway, in the middle: 5-LO/CysLTs cascade and the receptors, (AA is catalyzed by 5-LO/FLAP to form primary metabolite LTA4, and then converted to LTC4 via LTC4S (in leukocytes) or mGST2 (in a wide variety of cells). Subsequently, LTC4 exports from cells, and extracellularly cleaves and sequentially forms CysLTs), and in the right: LTB4 bypass.

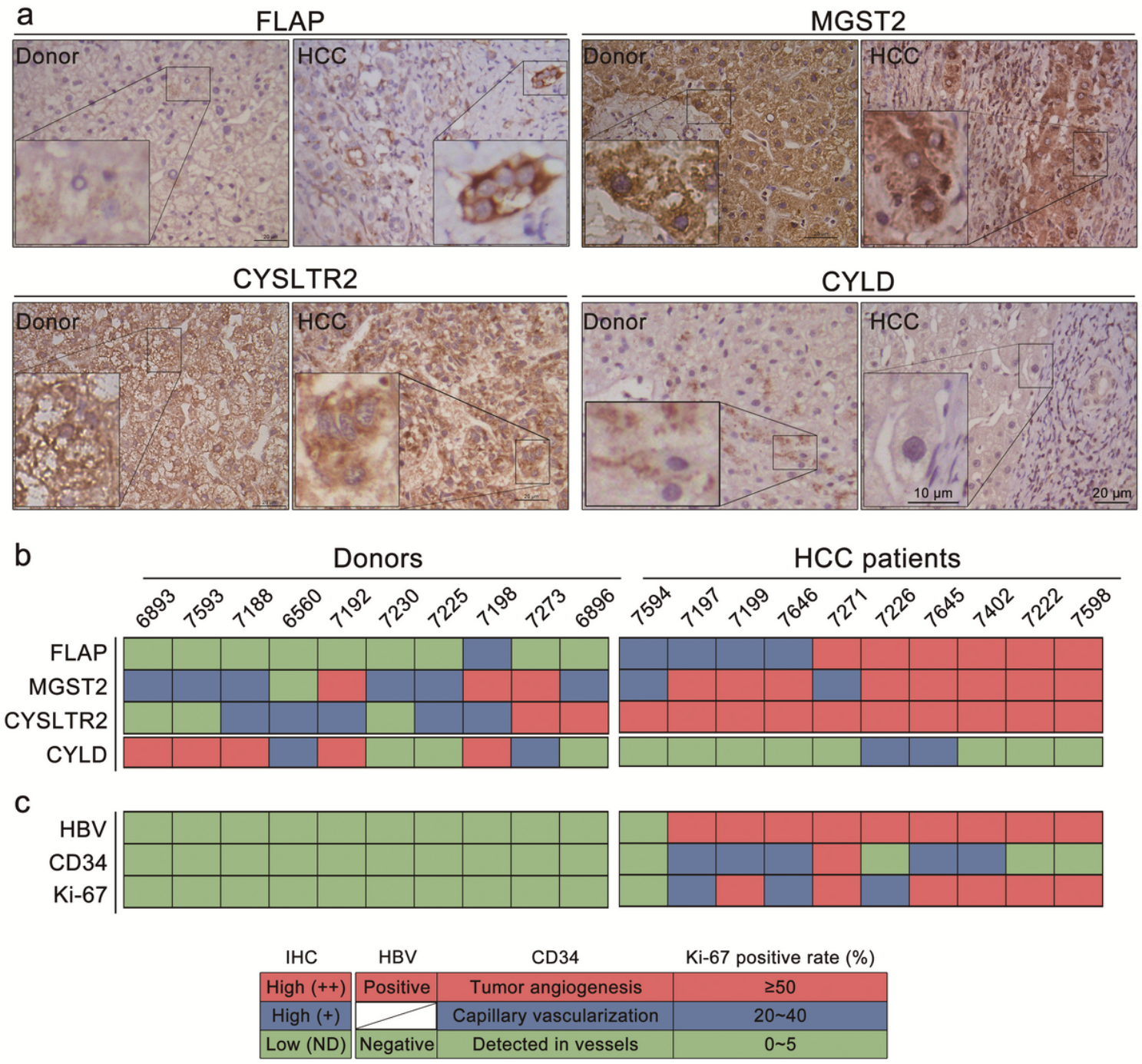

Figure 2

Overexpression of FLAP correlates to CYLD suppression in resection tissues of HCC patients. a. Representative immunohistochemistry (IHC) images of FLAP, MGST2, CysLTR2, and CYLD in each subject using indicated antibodies. Scale Bar=20 μm, bar=10 μm (magnification). b. The expression levels of FLAP, mGST2, CysLT2 and CYLD were clustered. Patient and donor codes are indicated. Grades of the indicated markers (Red: ++ = brown, Blue: + = golden, Green: ND = not detected). c. The expression levels of and positive rate (%) for CD34 localization and Ki-67 were clustered. Patient and donor codes are matched. For each analysis n=10/per group.

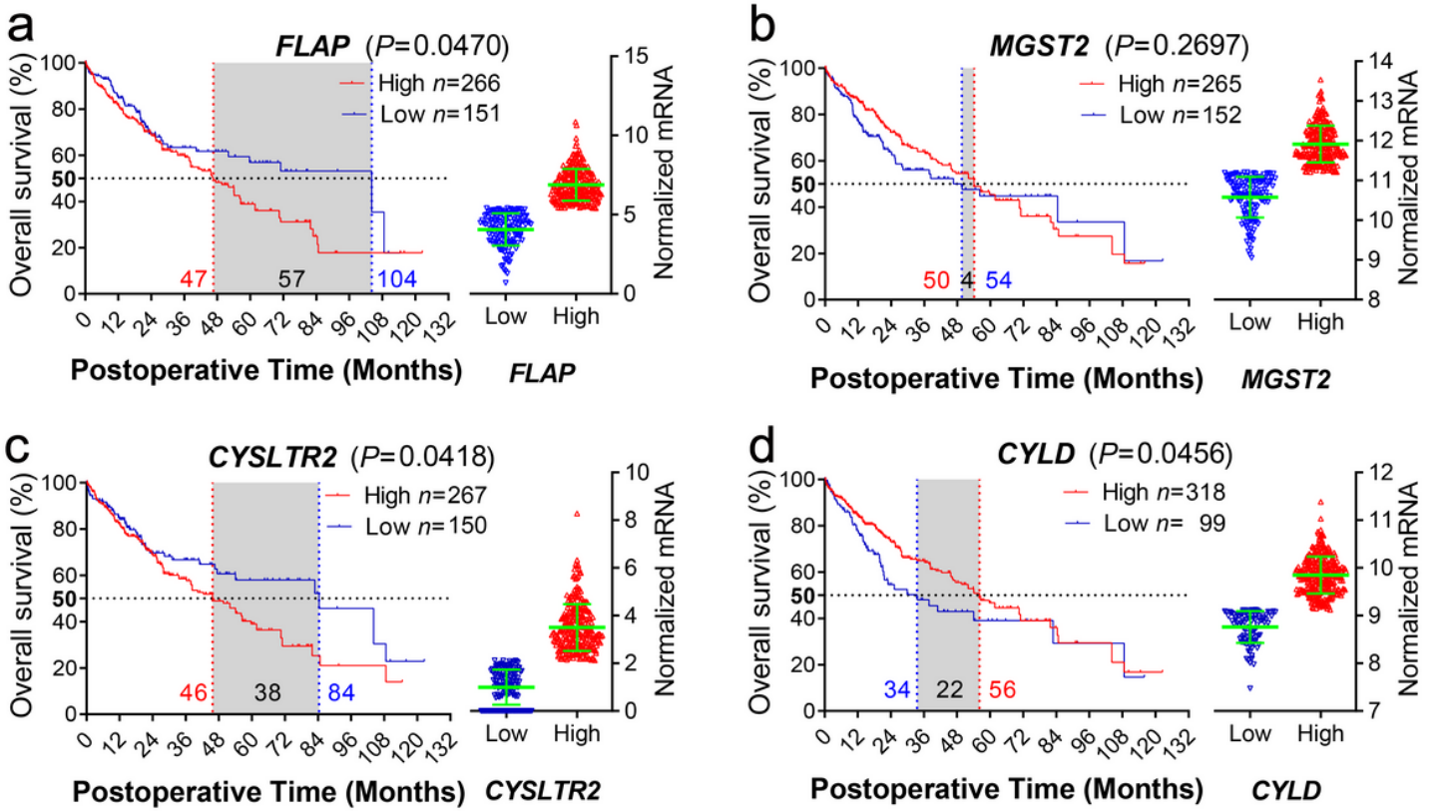

Figure 3

Enhanced hepatic FLAP mRNA shortens median survival time of HCC patients after surgical resection. Data for either HCC patients after HCC surgical resection or liver transplantation from the TCGA Research Network http://cancergenome.nih.gov/ were eligible for survival analysis. (a-d) Left panels: Kaplan-Meier survival curves in coordinate axis for comparing survival rates between high- and low- gene transcription subgroups from HCC cohort. Horizontal dotted line: 50% survival. Vertical red/blue dotted lines: median survival time (MST). a. FLAP mRNA (P=0.0470). b. mGST2 mRNA (P=0.2697). c. CysLTR2 mRNA (P=0.0418). d. CYLD mRNA (P=0.0456). Right panels: Scattered plots of transcription levels for indicating genes from HCC cohort. A Student unpaired U test was used to compare groups, and a P value less than 0.05 was considered statistically significant.

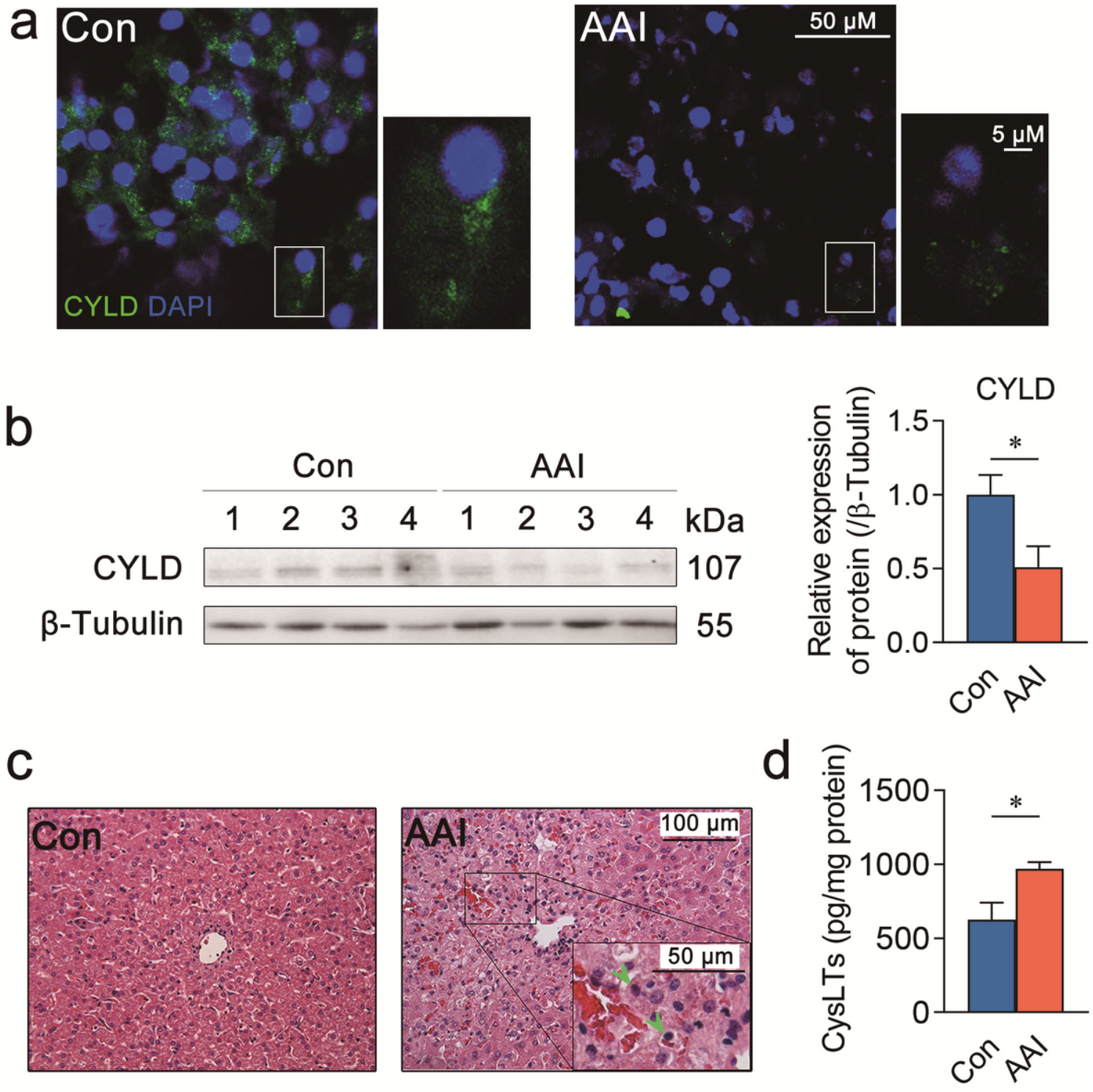

Figure 4

Hepatic CYLD attenuation is parallel to increased CysLTs production after AAI treatment in canines. Liver tissues were obtained from canines after treatment with AAI (3 mg/kg/day) or filler only (negative control, Con) for 10 days. a. Representative photomicrographs of CYLD (green: distributed in cytoplasm, DAPI: nuclei) in liver sections stained by immunofluorescence histochemistry. Bar=50 μm, bar=5μm (magnification). b. Immunoblot analysis displayed hepatic CYLD decreased in expression. β-Tubulin was used as an internal loading control. c. Representative photomicrographs of liver sections stained with

H&E (inflammatory cells, arrowheads). Bar=100 μm, bar=50 μm (magnification). c. Supernatant CysLTs level in liver tissue homogenate detected by ELISA. Error bars represent the mean value ± SD; A Student unpaired t test was used to compare groups, and a P value less than 0.05 was considered statistically significant. *P<0.05 vs control. For each analysis n=4/per group.

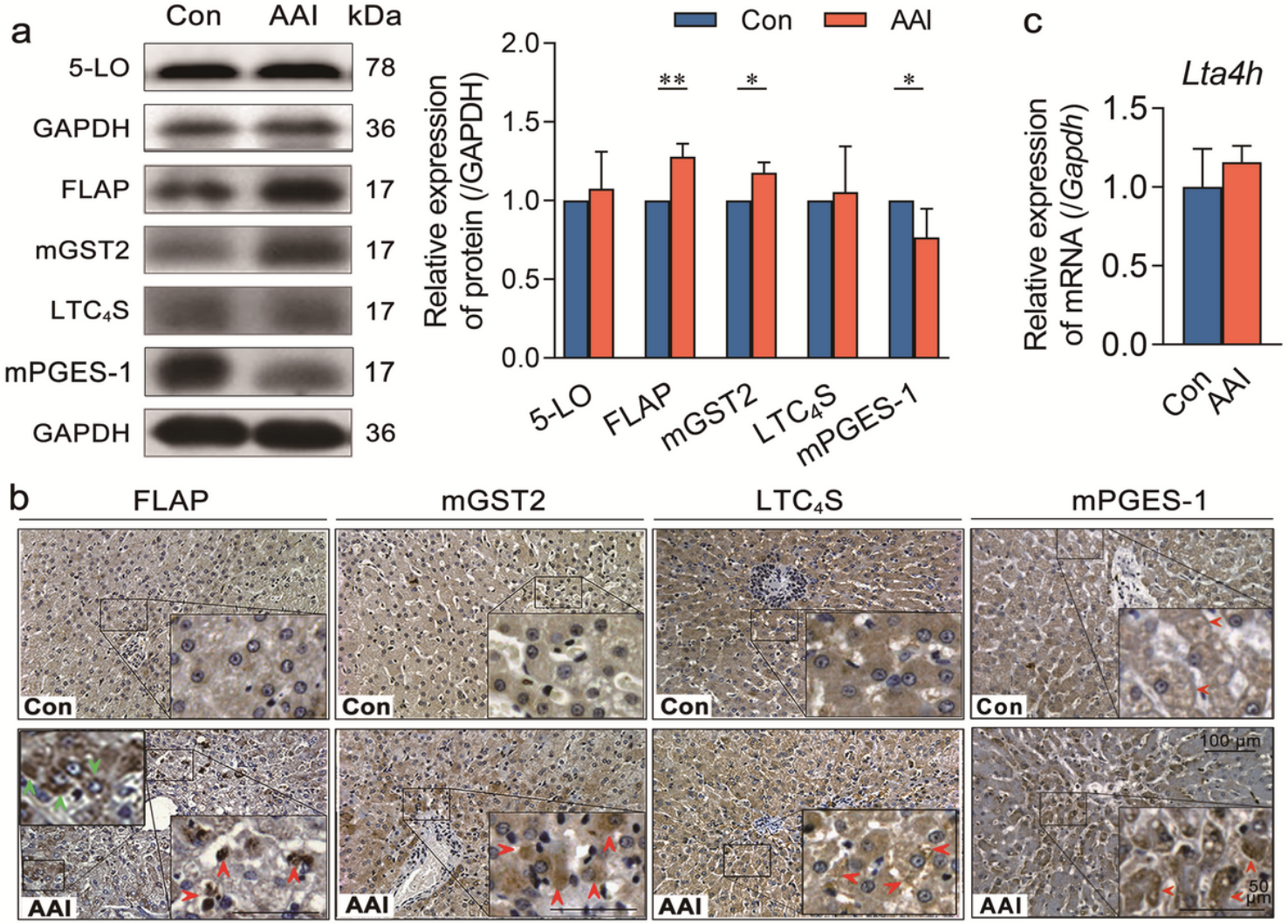

Figure 5

AAI treatment leads to FLAP overexpression in canine livers. Liver tissues were obtained from canines after treatment with AAI (3 mg/kg/day) or filler only (negative control, Con) for 10 days. a. Representative Western blotting of the catalytic proteins in 5-LO/CysLTs cascade. b. Representative photomicrographs with immunohistochemical stains using indicated antibodies. FLAP in hepatocytes (dark brown, green arrowheads) and Kupffer cells (dark brown, red arrowheads), mGST2 (light brown, arrowheads), CLT4S (arrowheads) in liver tissues. MPEGS-1 was also checked. Bar=100 μm, Bar=50 μm (magnification). c. The transcription of hepatic Lta4h was analyzed by real-time quantitative PCR. Error bars represent the mean value ± SD; A Student unpaired t test was used to compare groups, and a P value less than 0.05 was considered statistically significant. *P<0.05, **P< 0.01 vs control. For each analysis n=4/per group.

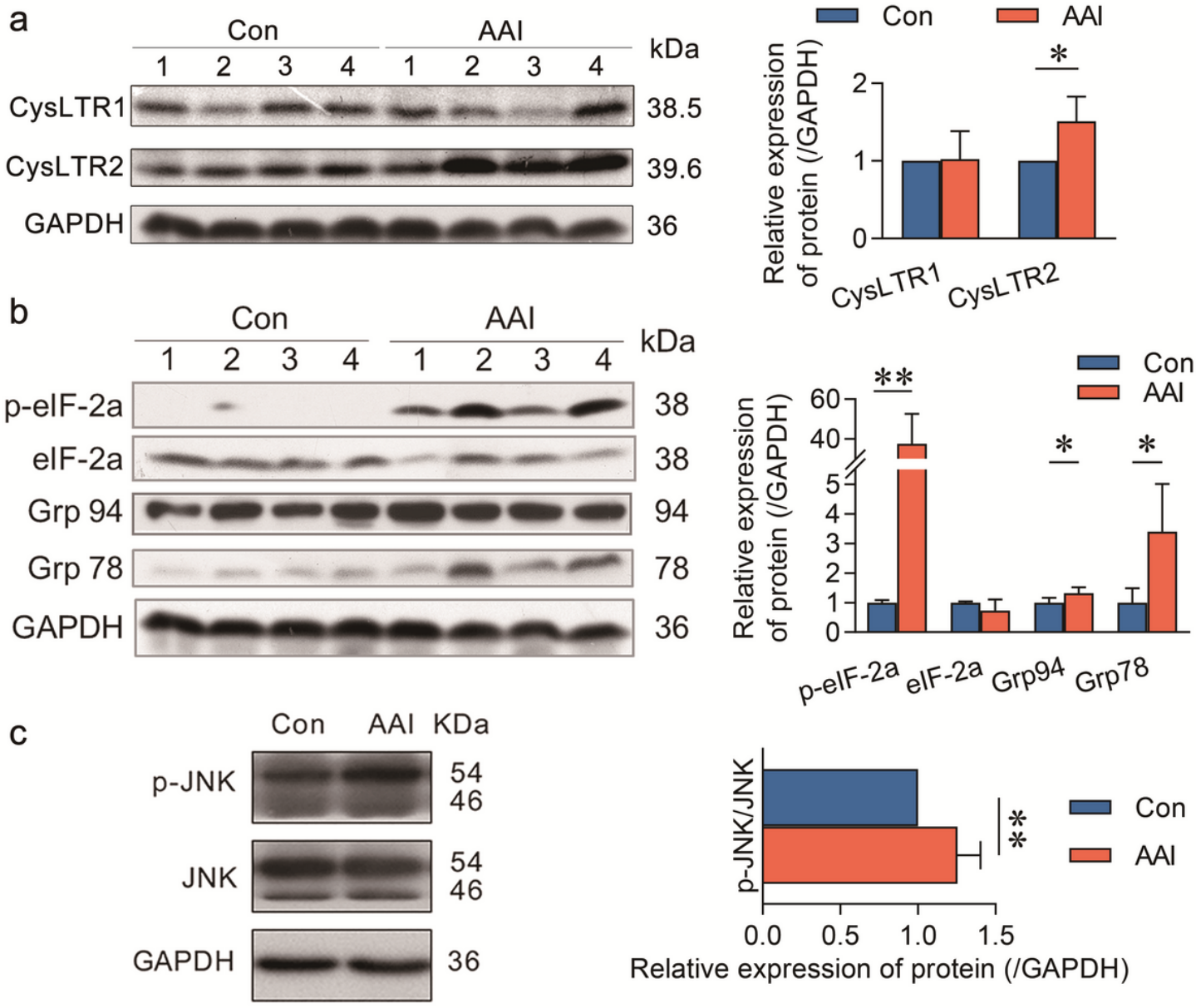

Figure 6

CysLTR2 overexpression along with ER stress and JNK phosphorylation in AAI-treated livers of canines. Liver tissues were obtained from canines after treatment with AAI (3 mg/kg/day) or filler only (negative control, Con) for 10 days. Immunoblot analyses of a. CysLTRs, b. molecular events for ER stress, and c. phosphorylated JNK. GAPDH was used as loading control. Error bars represent the mean value ± SD; A Student unpaired t test was used to compare groups, and a P value less than 0.05 was considered statistically significant. *P<0.05 vs control. **P< 0.01 vs control. For each analysis n=4/per group.

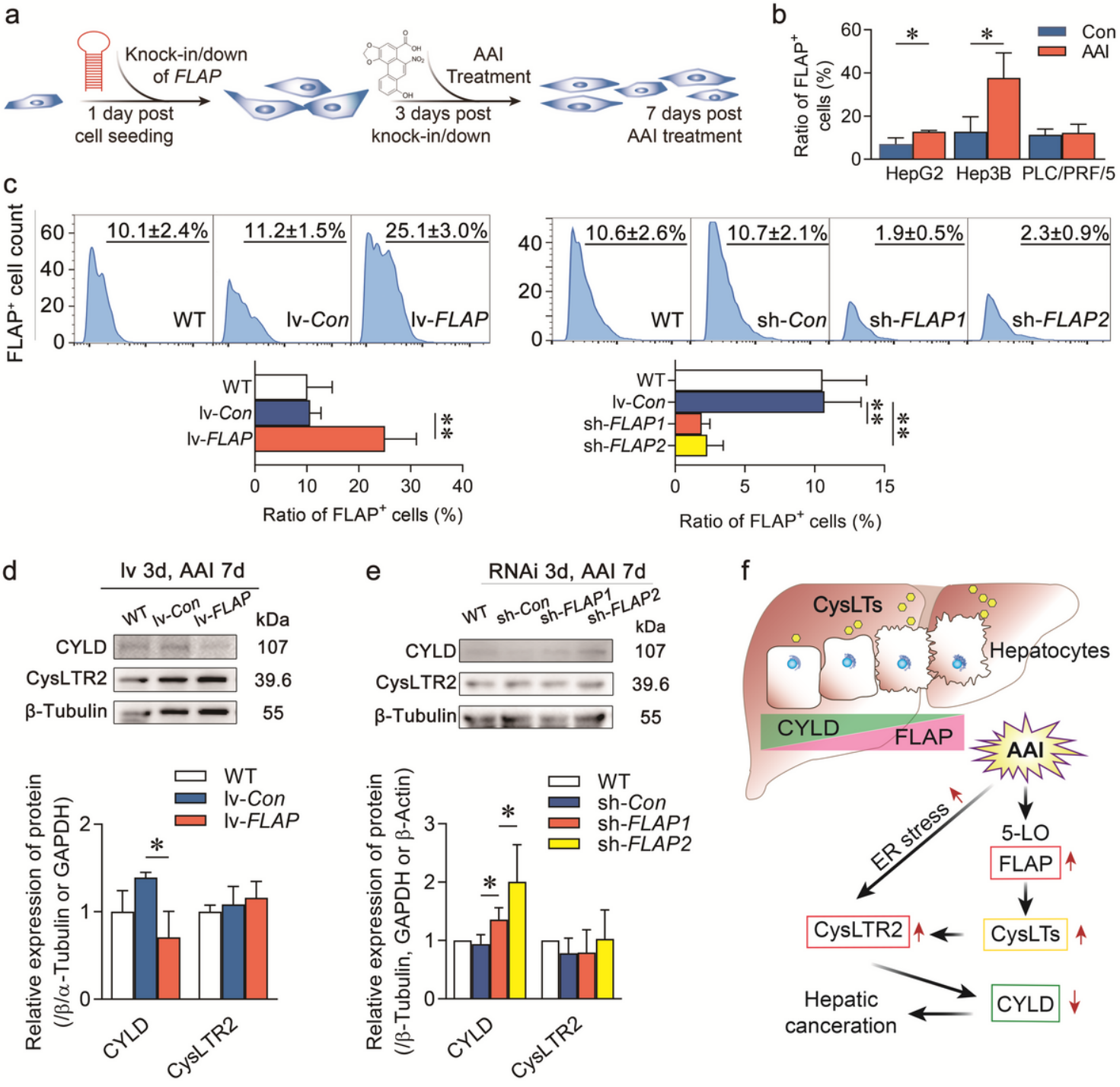

Figure 7

Overexpression of FLAP diminishes CYLD expression in HepG2lv-FLAP cells. a. Scheme of the experimental procedure. b. FLAP-positive (FLAP+) cell ratio in human HCC cell line HepG2, Hep3B2.1-7 and PLC/PRF/5 in response to AAI by flow cytometry assay, respectively. c. FLAP-positive (FLAP+) cell ratio in WT, HepG2lv-FLAP, and HepG2sh-FLAP cells by flow cytometry assay. d, e. Immunobloting analyses of CYLD and CysLTR2 in WT, HepG2lv-FLAP, or HepG2sh-FLAP cells. β-Tubulin was used as loading control. f. Schematic representation of FLAP overexpression results in CYLD attenuation in HCC

canceration process. Error bars, mean value ± SD; A Student unpaired t test was used to compare groups, and a P value less than 0.05 was considered statistically significant. *P< 0.05 vs control, **P< 0.01 vs control. For each analysis, n=3.

Supplementary Files

This is a list of supplementary files associated with this preprint. Click to download.

- AdditionalFile1SupplementaryTable1.doc
- AdditionalFile2SupplementaryTable2.doc
- AdditionalFile3SupplementaryTable3.doc
- AdditionalFile4FigureS1AAICysLTs.tif
- AdditionalFile5FigureS2humanIHC.tif
- AdditionalFile6FigureS3AAIBLTs.tif
- AdditionalFile7FigureS4Knock.tif